

Energy & Environmental Science

Accepted Manuscript



This is an *Accepted Manuscript*, which has been through the Royal Society of Chemistry peer review process and has been accepted for publication.

Accepted Manuscripts are published online shortly after acceptance, before technical editing, formatting and proof reading. Using this free service, authors can make their results available to the community, in citable form, before we publish the edited article. We will replace this *Accepted Manuscript* with the edited and formatted *Advance Article* as soon as it is available.

You can find more information about *Accepted Manuscripts* in the [Information for Authors](#).

Please note that technical editing may introduce minor changes to the text and/or graphics, which may alter content. The journal's standard [Terms & Conditions](#) and the [Ethical guidelines](#) still apply. In no event shall the Royal Society of Chemistry be held responsible for any errors or omissions in this *Accepted Manuscript* or any consequences arising from the use of any information it contains.

1 **Performance of a Mixing Entropy Battery Alternately**
2 **Flushed with Wastewater Effluent and Seawater for**
3 **Recovery of Salinity-gradient Energy**

4 Meng Ye,^{ad} Mauro Pasta,^b Xing Xie,^{ab} Yi Cui,^{bc*} Craig S. Criddle ^{*ad}

5

6 ^a*Department of Civil and Environmental Engineering, Stanford University, Stanford, California 94305,*
7 *USA.*

8 ^b*Department of Materials Science and Engineering, Stanford University, Stanford, California 94305,*
9 *USA.*

10 ^c*Stanford Institute for Materials and Energy Sciences, SLAC National Accelerator Laboratory, Menlo*
11 *Park, California 94025, USA.*

12 ^d*Woods Institute for the Environment and the Department of Civil and Environmental Engineering,*
13 *Stanford University, Stanford, California 94305, USA.*

14 *To whom correspondence should be addressed. E-mail: ccriddle@stanford.edu

15

16 **Salinity gradient energy, also referred to as *blue energy*, is a largely untapped source of**
17 **renewable energy. Coastal wastewater treatment plants discharge a continuous stream**
18 **of low salinity effluent to the ocean and are thus attractive locations for recovery of blue**
19 **energy. One method of tapping this gradient is a “*mixing entropy battery*” (MEB), a**
20 **battery equipped with anionic and cationic electrodes that charge when flushed with**
21 **freshwater and discharge when flushed with seawater. We constructed a plate-shape**
22 **MEB, where the anionic electrode was Ag/AgCl, and the cationic electrode was**
23 **Na₄Mn₉O₁₈ (NMO). Over a single cycle with a single cell, the net energy recovery was**
24 **0.11 kWh/m³ of wastewater effluent. When twelve cells were connected in series, the net**
25 **energy recovery (energy produced after subtracting energy invested) was 0.44 kWh/m³**
26 **of wastewater effluent. This is 68% of the theoretical recoverable energy of 0.65 kWh/m³**
27 **of wastewater effluent.. We conclude that (1) wastewater effluent can be effectively used**

1 for charging of a MEB, (2) cells in series are needed to optimize net energy recovery
2 efficiency, (3) there is a trade-off between net energy recovery efficiency and capital
3 investment, (4) there is a trade-off between net energy recovery efficiency and power
4 output, and (5) new electrode materials are needed to increase capacity, decrease cost,
5 and to avoid release of Ag to seawater.

6 Introduction

7 Current wastewater treatment is energy-intensive. Treatment of the 126 million cubic
8 meters of domestic wastewater generated each day in the United States accounts for
9 ~3% of the nation's electrical energy load¹. Similar values are reported for other
10 developed countries¹. But this should not be the case: the theoretical chemical energy
11 recoverable from organic matter and ammonium in the wastewater is ~1.5-2 kWh/m³,
12 about three times the electrical energy required for the treatment (~0.6 kWh/m³) (ref
13 2). Moreover, at many treatment plants, an untapped supply is the entropic energy
14 available when low salinity wastewater effluent discharges to a saline water body.
15 Theoretical calculations indicate that 0.65 kWh of energy can be recovered from
16 mixing of 1 m³ of wastewater effluent with seawater, an amount comparable to the
17 electrical energy currently consumed at wastewater treatment plants¹. Globally, the
18 potentially recoverable power at coastal treatment plants is estimated to be 18 GW (ref
19 3). If the chemical and entropic energies are both recovered, wastewater treatment
20 plants can become net power producers rather than consumers.

21

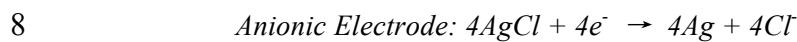
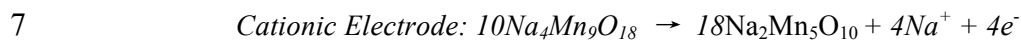
22 Others have investigated technologies for recovery of the entropic energy of mixing,
23 often referred to as "blue energy"⁴. Pressure retarded osmosis (PRO) and reverse
24 electro dialysis (RED) have received the most attention⁵⁻¹³. The main drawback of
25 these technologies is their use of membranes that are costly and prone to bio-fouling
26 and mechanical rupture³. To address these issues, researchers developed
27 membrane-less technologies, such as vapor compression¹⁴ and hydrocratic generator¹⁵.

1 These devices also have limitations: vapor compression and hydrocratic generators
2 are mechanically complex. Recently, a new series of techniques has been invented,
3 called “capacitive mixing”, for blue energy recovery^{16~18}. Three different types of
4 “capacitive mixing” processes have been studied, including capacitive double layer
5 expansion (CDLE) devices¹⁹, which store ions in the electric double-layer on the
6 porous electrode surface when an external voltage is applied^{19,20}, devices based on
7 capacitive Donnan potential (CDP)^{21,22,23}, which employ ion-selective membranes to
8 separate cations and anions, and mixing entropy batteries (MEBs)²⁴, which use battery
9 electrodes that store and release specific ions. All processes involve a four-step cycle
10 to extract energy from salinity gradients. An optimal cycle, in analogy to the Carnot
11 cycle, is proposed to maximize energy recovery for these four-step cycles²⁵. Each
12 technique has a reverse process for desalination: capacitive deionization (CDI) is the
13 reverse of CDLE^{26,27}; membrane capacitive deionization (MCDI) is the reverse of
14 CDP^{28~30}; and a desalination battery reverses the process used in a MEB^{24,31}. The
15 MEB is a promising technology because it uses battery electrodes with relatively high
16 specific capacity and low self-discharge. In the proof-of-concept study²⁴, a high
17 efficiency of energy extraction (74%) was inferred based on overpotentials with a
18 single pair of electrodes. Net energy recovery efficiency was not directly measured,
19 and operational factors affecting efficiency were not explored. In a previous study, we
20 evaluated the potential of MEBs for recovery of blue energy from lake water and
21 seawater salt gradients²⁴. This proof-of-concept study entailed use of $\text{Na}_2\text{Mn}_5\text{O}_{10}$ and
22 commercially available silver nanoparticles as the cationic and anionic electrodes. In
23 this study, we evaluate the potential for recovery of blue energy at coastal wastewater
24 treatment plants. We test treated wastewater effluent and seawater and change the
25 cationic electrode material to a higher capacity material - $\text{Na}_4\text{Mn}_9\text{O}_{18}$ (NMO)
26 (compared with $\text{Na}_2\text{Mn}_5\text{O}_{10}$ used in our previous work^{24,31}). We investigate the
27 potentials and limitations of these materials for this application. More importantly, we
28 seek to identify process design trade-offs that must be considered regardless of the

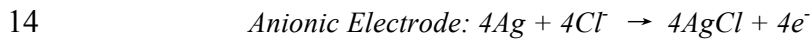
1 electrode materials used.

2 **Results and Discussion**

3 Figure 1 illustrates the four-step cycle of the MEB first demonstrated in a previous
4 proof-of-concept study²⁴. In the presence of low salinity wastewater effluent, power is
5 supplied at a constant current, releasing Na^+ from the cationic electrode and Cl^- from
6 the anionic electrode. During this charge step, the reactions are:



9 When this solution is replaced by seawater, the voltage between the electrodes
10 increases due to the increase in NaCl concentration, current reverses direction, and
11 power is generated as Na^+ and Cl^- ions are reincorporated into the electrodes. During
12 this discharge step, the net reactions are:



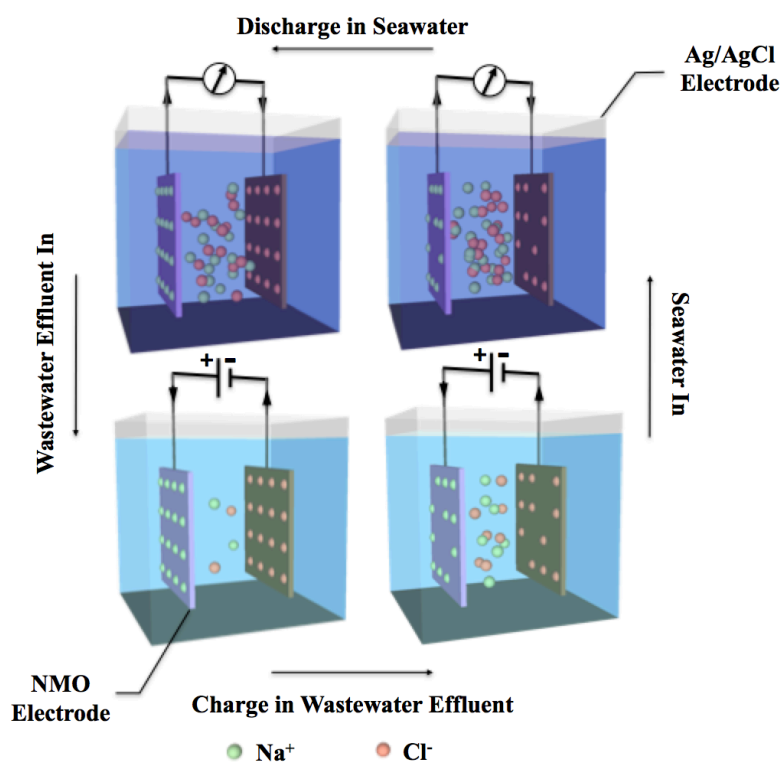
15 The net energy produced in each cycle is the path integral of the potential vs. charge
16 curve. Energy out exceeds energy in because the battery is charged at a lower voltage (in
17 wastewater effluent) and discharged at a higher voltage (in seawater). This process is made
18 possible because charge and discharge occur at different NaCl concentrations. The additional
19 energy is generated through the mixing of dilute wastewater effluent and seawater.

20

21 For these experiments, we used wastewater effluent from the Palo Alto Regional
22 Water Quality Control Plant. The NaCl concentration of this solution is 0.032 M, a
23 concentration that is a little higher than that of a typical river or lake. Seawater with a
24 NaCl concentration of 0.6 M was obtained at Half Moon Bay, CA. Water samples were
25 collected in plastic bottles, sealed, and stored at 4°C. Initial battery voltages were
26 reproducible, indicating stable ionic strength for all experiments. Both the wastewater
27 effluent and seawater were used directly without pretreatment. Details of the

1 processes used to synthesize electrodes are described in the Supplementary
 2 Information. The electrodes were pre-cycled (Fig. S2 and Fig. S3) and then installed
 3 parallel to one another at a 1.7 mm distance in a 1.5 mL plate-shape cell. The internal
 4 resistance of the device was measured by potentiostatic impedance spectroscopy.
 5 Because the distance between electrodes was small, internal resistance was low: 17 Ω
 6 for wastewater effluent and 3 Ω for seawater.

7



8

9 **Figure 1** Work cycle for a mixing entropy battery. In the bottom half of the figure,
 10 wastewater effluent flushes the cell and a current is applied (current direction is right
 11 to left) in order to charge the battery. Ions in the electrodes are released into solution.
 12 In the top half of the figure, seawater flushes the cell and energy is recovered (current
 13 direction is left to right) as the battery discharges. Ions in the seawater enter the
 14 electrodes. For the charge step, the *cationic electrode half reaction* is: $10\text{Na}_4\text{Mn}_9\text{O}_{18}$
 15 $\rightarrow 18\text{Na}_2\text{Mn}_5\text{O}_{10} + 4\text{Na}^+ + 4\text{e}^-$; the *anionic electrode half reaction* is: $4\text{AgCl} + 4\text{e}^-$
 16 $\rightarrow 4\text{Ag} + 4\text{Cl}^-$. For the discharge step, these reactions run in reverse.

17

1 The theoretically extractable blue energy was¹³:

$$\Delta G_{\text{mix}} = 2RT[V_E C_E \ln \frac{C_E}{C_M} + V_S C_S \ln \frac{C_S}{C_M}]$$

2 where C_E is the NaCl concentration in the wastewater effluent, C_S the NaCl
3 concentration in seawater, V_E the volume of wastewater effluent, V_S the volume of
4 seawater, R the universal gas constant, and T the absolute temperature. C_M is the
5 NaCl concentration after complete mixing of wastewater effluent and seawater:

$$C_M = \frac{V_E C_E + V_S C_S}{V_E + V_S}$$

6 This is an approximation because activity coefficients are assumed equal to unity, and
7 the entropy increase of water is neglected. When these factors are considered, they
8 counterbalance one another¹³. Because wastewater effluent is the limiting resource,
9 the key performance metric is energy production per unit volume of effluent. When
10 $V_S \gg V_E$ (i.e. wastewater effluent is mixed with an infinite volume of seawater),
11 $\Delta G_{\text{mix}}/V_E$ approaches 0.65 kWh/m³ of wastewater effluent, the theoretical extractable
12 free energy (Supplementary Information).

13

14 In order to simulate cells in series, we recycled wastewater effluent (1.5 mL) back to a single
15 cell, and applied a current to charge the cell. After completing this charge step, we removed
16 the wastewater effluent, and reused it on the charge step in the next cycle. In the discharge
17 step for every cycle, we flushed the cell with seawater. By repeating this cycle 12 times, we
18 simulated 12 cells in series. The wastewater effluent became progressively more saline
19 with each successive cycle. The current applied in the charge step of each cycle was
20 0.25 mA. The discharge current was also 0.25 mA, but in the reverse direction. The
21 time for charge and discharge was 6 hours, giving a total cycle time of 12 hours. The
22 HRT of wastewater effluent was 72 hours through 12 cycles. This HRT can be
23 decreased by increasing the surface area of electrode exposed to flow or by increasing
24 current density. We limited the number of cycles to 12 because the energy loss in the
25 thirteenth cycle exceeded the energy available from the salinity gradient. The volume

1 of seawater added to reach this point was 12 times the volume of the original
2 wastewater effluent.

3

4 To assess voltage losses, we define a “voltage ratio” as the observed voltage rise
5 when seawater (0.6M) displaces freshwater (0.032M) divided by the theoretical
6 voltage rise calculated from the known salinity gradient (expressed as a percentage).

7 We used the Nernst equation to calculate the theoretical voltage rise (ranges from 0.11
8 to 0.15 V depending upon cycle time) from the known concentration of NaCl in

9 seawater and the calculated salt concentration in salinated wastewater effluent after
10 charging (see Supplementary Information for detailed calculation). We calculate the

11 salt concentration after charging as the concentration of the wastewater effluent prior
12 to charging (0.032 M) plus the increase in concentration from added charge (current

13 times time). As shown in Fig. 2A, the voltage ratio decreased from 87% in the first
14 cell to 64% in the final cycle. This is because the theoretical voltage rise decreases as

15 the salinity gradient decreases. After the sixth cycle, voltage ratio stabilized: the
16 decrease in voltage loss due to increased electrolyte salinity (and therefore

17 conductivity) compensated for a decrease in the salinity gradient. Fig. 2B shows the
18 net energy production and net power output per unit area of electrode per cycle. When

19 the salinity gradient is high, the net energy recovered from the first cycle was 0.11
20 kWh/m³ of wastewater effluent, about 17% of the theoretically available energy. Net

21 energy recovery from the final cycle was only 0.01 kWh/m³ of wastewater effluent.
22 The decrease in the salinity gradient allowed little energy recovery despite a voltage

23 ratio of 64%. Net power output per unit area of electrode per cycle decreased from
24 10.4 to 0.6 mW/m².

25

26 Figure 2C illustrates the cumulative energy production and the overall energy
27 efficiency for 12 cycles. Cumulative energy production is the sum of energy

28 recoveries for individual cycles. Overall energy efficiency is cumulative energy

1 production divided by the theoretical free energy of 0.65 kWh/m³ of wastewater
2 effluent. Cumulative energy production was 0.44 kWh/m³ of wastewater effluent, and
3 the overall energy efficiency was 68%. Theoretically, reuse of a given volume of
4 wastewater effluent in an infinite number of cycles would maximize energy
5 production per unit volume of wastewater effluent. However, there is a trade-off
6 between net energy recovery and average power output. As the number of cycles
7 increases, net energy recovery efficiency increases but average power output
8 decreases (Fig. 2D). Moreover, in real world applications, use of more cycles results
9 in a higher capital cost because more electrode surface area is needed and/or more
10 energy is invested for recycling of wastewater effluent. As shown in Fig. 2C, an
11 efficiency of 60% can be achieved with 8 cycles in series. Increasing the number of
12 cycles from 8 to 12 increases the energy efficiency by just 10%. These trade-offs are
13 clearly important for future economic analyses.

14

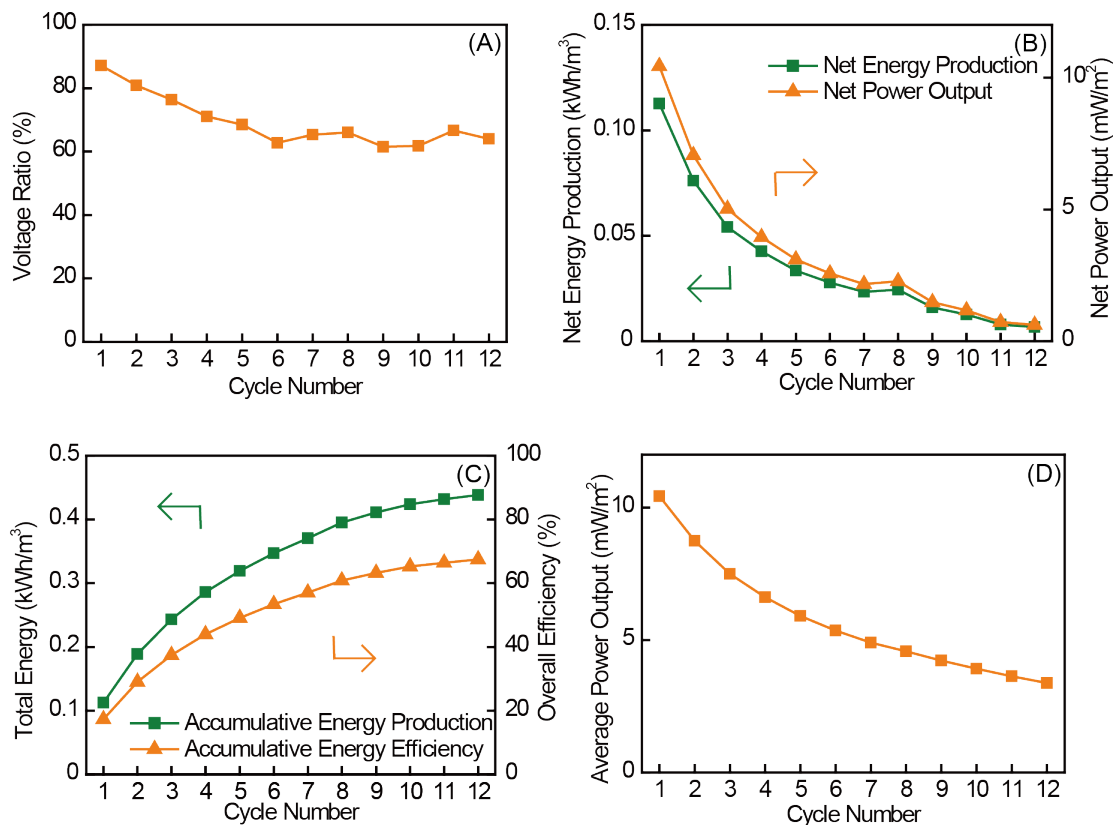
15 In order to optimize the energy recovery by MEBs, we investigated several
16 operational parameters. The first was the charge exchanged during the charge and
17 discharge steps. The experiments were conducted by varying the cycle time from 40
18 minutes to 12 hours at a current of 0.25 mA. The path integral of the potential vs.
19 charge curve indicates the net energy production from each cycle (Fig. 3A). More
20 energy is extracted from a cycle when more charge is exchanged by extending the
21 cycle time. Figure 3B and Fig. S8 (plot the observed voltage rise verses theoretical
22 voltage rise) illustrate the theoretical voltage rise, overpotential, and observed voltage
23 rise as a function of cycle time. The theoretical voltage rise decreases from 0.15 to
24 0.11 V with cycle time. As cycle time increases, more electron equivalents are
25 exchanged. This is because the current is constant ($Q_{Transferred} = Current \cdot t_{Cycle}$).
26 Exchange of more electron equivalents drives exchange of ions from the electrodes
27 into solution. Exchange of more ions results in a lower voltage rise as cycle time
28 increases, decreasing the gradient for energy recovery. As shown in Fig. 3B and Fig.

1 S8, the theoretical voltage rise is close to the observed voltage rise, reflecting a low
2 and stable overpotential. High and stable voltage ratio (91% to 88%) was observed
3 (Fig. S6). Figure 3C shows increasing energy production per cycle with increased
4 cycle time (i.e., charge transferred). Energy production increased approximately
5 linearly from 0.01 kWh/m³ of wastewater effluent to 0.10 kWh/m³ of wastewater
6 effluent with increased cycle time (i.e., charge exchanged). Ultimately, specific
7 capacity of the electrode material becomes a limiting factor. Substantial energy loss
8 resulted when the cycle time increased to 20 hours, and the charge curve crossed the
9 discharge curve (Fig. S4). The cycle time is thus limited by the capacity of the
10 cationic electrode material (details in Supplementary Information). Because only a
11 portion of the capacity of the material can be used, more cells and material are
12 required to achieve efficient energy recovery. Materials with higher specific capacity
13 are desirable.

14

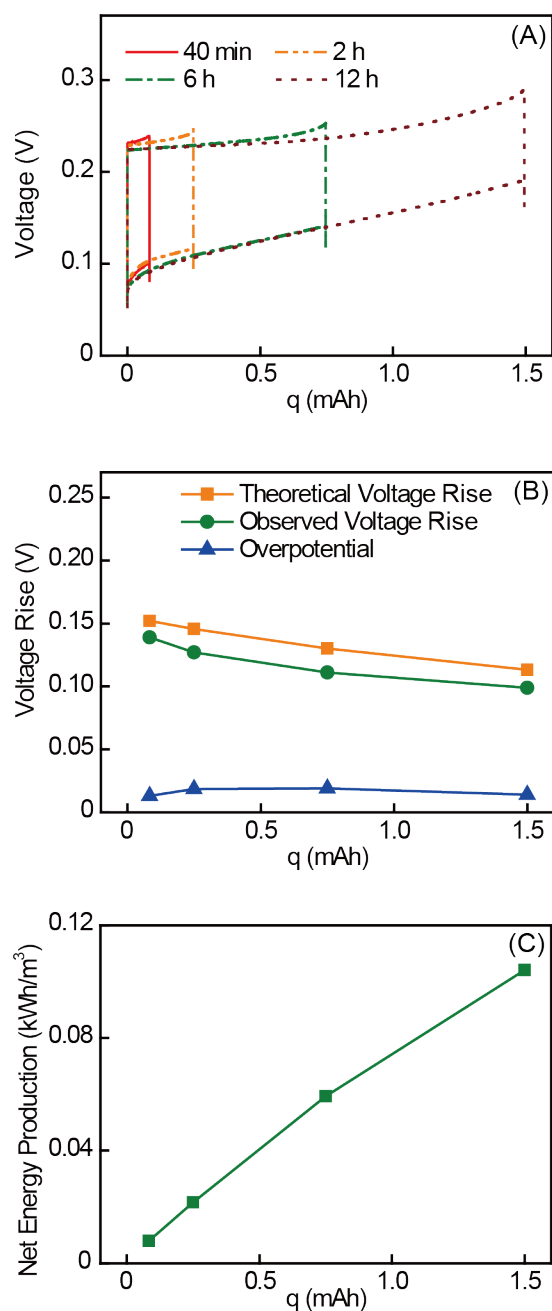
15 Another parameter that affects MEB performance is the current applied during the
16 charge and discharge steps. To evaluate this variable, we fixed the total amount of
17 charge at 1.5 mAh and evaluated 8 different currents ranging from 0.125 mA to 1 mA.
18 As we increased the current applied, the quadrangle defined by the path integral of
19 each charge-discharge cycle shrank along the Y-axis (Fig. 4A). This indicates a
20 decrease in net energy production. Figure 4B illustrates the voltage profiles for each
21 cycle at different applied currents. The theoretical voltage rise did not change because
22 the number of charges exchanged was fixed. Concentration differences between
23 salinated wastewater effluent and seawater were the same for all cases. On the other
24 hand, the overpotential increased almost linearly with current, resulting in a decrease
25 in the observed voltage rise. The voltage ratio decreased from 98% to 42% (Fig. S7).
26 Figure 4C shows the energy production of each cycle. The energy production
27 decreased from 0.12 kWh/m³ to 0.04 kWh/m³ (Fig. 4C). When higher currents are
28 applied, overpotentials increase and eventually exceed the voltage rise resulting from

1 the concentration difference between wastewater effluent and seawater. No energy
 2 can be recovered. Clearly, this is a condition to be avoided. As noted above,
 3 increasing the applied current decreases efficiency and energy production, but high
 4 applied current is needed to give high power output per cell. Furthermore, if the
 5 amount of effluent discharged by a wastewater treatment plant is fixed, the number of
 6 charges needed to salinate the effluent remains constant. With the current applied per
 7 cell is low, more cells are required, and the capital investment increases. Calculations
 8 are needed to determine the optimal trade-off, providing energy efficiency and power
 9 output with the minimum capital investment.



10
 11 **Figure 2** Energy extraction from 12 mixing entropy battery cycles using recycled
 12 wastewater effluent. (A) Voltage ratio for each cycle through the series of cycles. (B)
 13 Net energy production and net power output from each cycle through the series of
 14 cells. (C) Total energy production and overall energy efficiency through the series of
 15 cells. (D) Average power output with different number of cycles.

16



1

2 **Figure 3** Cycles with different amount of charges exchanged at a current of 0.25 mA.

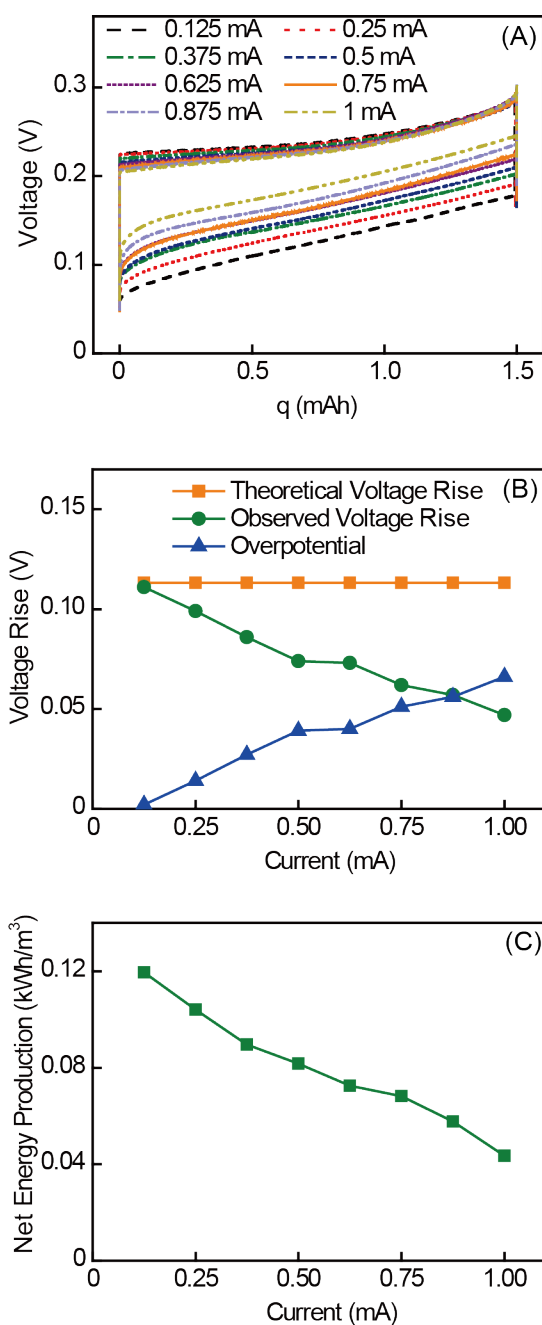
3 (A) Plot of voltage vs. charge showing energy extraction at cycle times of 40 min, 2 h,

4 6 h, and 12 h. (B) Voltage profile of cycles with different cycle time showing the

5 theoretical voltage rise, observed voltage rise, and overpotential in each cycle. (C) Net

6 energy production from each cycle for different cycle time.

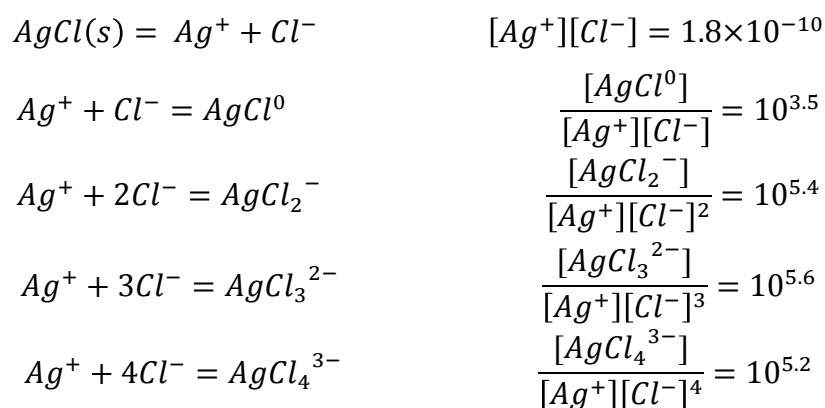
7



1

2 **Figure 4** Cycles at different current with a fixed amount of charge exchanged (1.5
 3 mAh). (A) Energy extraction cycles of mixing entropy batteries at current values
 4 ranging from 0.125 mA to 1 mA in a voltage vs. charge plot. As current increases, the
 5 quadrangle becomes smaller, indicating that less energy is recovered. (B) Voltage
 6 profile of cycles at different current showing the theoretical voltage rise, observed
 7 voltage rise, and overpotential in each cycle. (C) Net energy production from each
 8 cycle at different applied currents.

1 Long-term performance of MEBs using Ag/AgCl and NMO electrodes has been
 2 tested previously. Performance was stable over 100 cycles²⁴. But silver solubility is an
 3 issue: in seawater, soluble Ag complexes form with chloride. Because Cl⁻
 4 concentration could be as high as 0.6 M in seawater, considerable silver can dissolve
 5 during cycling. The relevant reactions and equilibrium constants are:



6 Neglecting the influence of applied current, the equilibrium concentration of total
 7 soluble silver forms is 8.9 ppm, almost 100 times the U.S. EPA secondary drinking
 8 water standard of 0.1 ppm³². Silver is known to cause adverse health effects including
 9 argyria, argyrosis, liver and kidney damage³³. After 12 hours of cycling, the measured
 10 soluble silver concentration in the wastewater effluent was 0.02 ppm and the
 11 concentration in the seawater was 0.9 ppm, still an order of magnitude above the EPA
 12 standard. Dissolution of silver also increases cost and decreases electrode cycle life.
 13 The average loading of the silver electrode is 0.01 g/cm², giving an estimated cycle
 14 life of about 7 years with constantly capacity loss for a Ag/AgCl electrode (based on
 15 the measured dissolution of 0.92 ppm Ag in 1.5 mL of solution over a 12 hours cycle).
 16 Ag/AgCl electrode was used in this study because its half reaction potential remains
 17 stable when oxidized or reduced. However, this analysis indicates that more stable
 18 and cheaper anionic electrode materials are needed. Preliminary results show that
 19 some conductive polymers will be acceptable as anionic electrode materials in MEBs.

20

1 **Conclusion**

2 This work establishes that a plate-shape MEB cell can enable a high efficiency of
3 energy recovery from domestic wastewater effluent and seawater. An overall
4 efficiency of 68% was achieved by charging the battery with 12 flushes of recycled
5 wastewater effluent. This demonstrates the potential for recovery of blue energy at
6 coastal wastewater treatment plants. To achieve high net energy recovery efficiencies,
7 cells in series are needed. This results in a trade-off between net energy recovery efficiency
8 and capital investment. We also observe a trade-off between power output and net energy
9 recovery efficiency. These conclusions are independent of the material tested and will
10 be broadly applicable for future optimization efforts where different users may assign
11 different relative weightings to net energy recovery efficiency, capital investment, and
12 power output. The actual net energy recovery efficiency will also depend upon local
13 conditions, such as requirements for pretreatment and pumping. Finally, this work
14 clarifies electrode material properties that would be desirable for practical application. The
15 ideal MEB electrode materials would enable a rapid potential response to changes in
16 the concentrations of Na^+ and Cl^- ; remain stable in wastewater effluent and seawater
17 over many cycles; and be abundant and cheap.

18 **Acknowledgement**

19 Support for this research was provided by the Woods Institute for the Environment at
20 Stanford University and by the U.S. NSF Engineering Research Center Re-inventing
21 the Nation's Urban Water Infrastructure. Support for X. X. was provided by a
22 Stanford Interdisciplinary Graduate Fellowship; support for M. P. was provided by
23 the Oronzio and Niccolò de Nora Foundation.

24

25

1 **References**

- 2 1 P. L. McCarty, J. Bae, J. Kim, *Environ. Sci. & Technol.*, 2011, **45**, 7100.
- 3 2 E. S. Heidrich, T. P. Curtis, J. Dolfing, *Environ. Sci. & Technol.*, 2011, **45**, 827.
- 4 3 B. E. Logan, M. Elimelech, *Nature*, 2012, **488**, 313.
- 5 4 J. W. Post, Blue Energy: electricity production from salinity gradients by reverse
6 electro dialysis, 2009.
- 7 5 O. Levenspiel, N. De Nevers, *Science*, 1974, **183**, 157.
- 8 6 S. Loeb, *J. Memb. Sci.*, 1976, **1**, 49.
- 9 7 S. E. Skilhagen, J. E. Dugstad, R. J. Aaberg, *Desalination*, 2008, **220**, 476.
- 10 8 T. Thorsen, T. Holt, *J. Memb. Sci.*, 2009, **335**, 103.
- 11 9 R. E. Pattle, *Nature*, 1954, **174**, 660.
- 12 10 J. N. Wienstein, F. B. Leitz, *Science*, 1976, **191**, 557.
- 13 11 R. E. Lacey, *Ocean Eng.* 1980, **7**, 1.
- 14 12 J. W. Post, H. V. M. Hamelers, C. J. N. Buisman, *Environ. Sci. & Technol.*, 2008, **42**,
15 5785.
- 16 13 J. Veerman, M. Saakes, S. J. Metz, G. J. Harmsen, *J. Memb. Sci.*, 2009, **327**, 136.
- 17 14 M. Olsson, G. L. Wick, J. D. Isaacs, *Science*, 1979, **206**, 452.
- 18 15 W. Finley, E. Pscheidt, *US Patent 6,313,545*, 2001.
- 19 16 D. Brogioli, R. Ziano, R. A. Rica, D. Salerno, O. Kozynchenko, H. V. M. Hamelers, F.
20 Mantegazza, *Energy Environ. Sci.*, 2012, **5**, 9870.
- 21 17 R. A. Rica, R. Ziano, D. Salerno, F. Mantegazza, R. V. Roij, D. Brogioli, *Entropy*,
22 2013, **15**, 1388.
- 23 18 M. F. M. Bijmans, O. S. Burheim, M. Bryjak, A. Delgado, P. Hack, F. Mantegazza, S.
24 Tenisson, H. V. M. Hamelers, *Energy Procedia*, 2012, **20**, 108.
- 25 19 D. Brogioli, *Physical Review Letters*, 2009, **103**, 058501.
- 26 20 D. Brogioli, R. Zhao, P. M. Biesheuvel, *Energy Environ. Sci.*, 2011, **4**, 772.
- 27 21 B. B. Sales, M. Saakes, J. W. Post, C. J. N. Buisman, P. M. Biesheuvel, H. V. M.

- 1 Hamelers, *Environ. Sci. & Technol.*, 2010, **44**, 5661.
- 2 22 F. Liu, O. Schaetzel, B. B. Sales, M. Saakes, C. J. N. Buisman, H. V. M. Hamelers,
3 *Energy Environ. Sci.*, 2012, **5**, 8642.
- 4 23 M. C. Hatzell, R. D. Cusick, B. E. Logan, *Energy Environ. Sci.*, 2014, **7**, 1159.
- 5 24 F. La Mantia, M. Pasta, H. D. Deshazer, B. E. Logan, Y. Cui, *Nano Lett.*, 2011, **11**,
6 1810.
- 7 25 N. Boon, R. Roij, *Mol. Phys.*, 2011, **109**, 1229.
- 8 26 Y. Oren, *Desalination*, 2008, **228**, 10.
- 9 27 S. Porada, R. Zhao, A. van der Wal, V. Presser, P. M. Biesheuvel, *Progress in*
10 *Materials Science*, 2013, **58**, 1388.
- 11 28 J. B. Lee, K. K. Park, H. M. Eum, C. W. Lee, *Desalination*, 2006, **196**, 125.
- 12 29 S. Jeon, H. Park, J. Yeo, S. Yang, C. H. Cho, M. H. Han, D. K. Kim, *Energy Environ.*
13 *Sci.*, 2013, **6**, 1471.
- 14 30 R. Zhao, O. Satpradit, H. H. M. Rijnaarts, P. M. Biesheuvel, A. van der Wal, *Water*
15 *Research*, 2013, **47**, 1941.
- 16 31 M. Pasta, C. D. Wessells, Y. Cui, F. La Mantia, *Nano Lett.* , 2012, **12**, 839.
- 17 32 U. S. EPA, *National Secondary Drinking Water Regulations*, 1979.
- 18 33 P. L. Drake, K. J. Hazelwood, *Ann. Occup. Hyg.*, 2005, **49**, 575.